Supporting Information

Theoretical Study of CDW phases for bulk NbX_2(X= S and Se)

Hongwei Du[1], Zhenyi Jiang[1*], Jiming Zheng[1*], Xiaodong Zhang[1], Wenxuan Wang[1], Zhiyong Zhang[2]

[1]Shaanxi Key Laboratory for Theoretical Physics Frontiers, Institute of Modern Physics, Northwest University, Xi'an 710069

[2]Stanford Research Computing Center, Stanford University, Stanford, CA 94305, United States

Section 1: Figure and Table

Table S-1 Lattice constants (Å) of bulk 2H-NbX_2 (X= S and Se) with various vdW corrections.

	No-vdW(S/Se)	D3(S/Se)	optB88b(S/Se)	optB86b(S/Se)	Exp(S/Se) [1,2]	Exp(S/Se) [3,4]
a	3.438 / 3.474	3.320 / 3.449	3.353 / 3.485	3.325 / 3.455	3.310 /3.443	3.418 / 3.449
c	13.227/ 13.932	11.773 / 12.303	12.011 / 12.646	11.816 / 12.501	11.890 / 12.547	11.860 / 12.546
c/a	3.847 / 4.010	3.546 / 3.567	3.582 / 3.629	3.554 / 3.618	3.592 / 3.644	3.470 / 3.638

Table S-2 Formation energies ΔE_{CDW} (meV/CDW) of CDW configurations (Nb_9X_{18}) for bulk 1H-NbX_2 (X= S and Se) with PBE, PBE+D3, and PBE+optB86b corrections.

Configuration	PBE(S/Se) (meV/CDW)	PBE+D3(S/Se) (meV/CDW)	PBE+optB86b(S/Se) (meV/CDW)
T	-26 / -36	-26 / -42	-29 / -45
Ts	-23 / -29	-24 / -39	-27 / -36
H	-19 / -25	-21 / -28	-24 / -32
S	-18 / -17	-19 / -22	-22 / -23

Table S-3 Lattice parameters (Å/ Å^3), total energy without vdW correction, and vdW of CDW and metal phase with the same number of atoms for bulk 2H-NbX_2 (X = S and Se)

	a	*b*	*c*	*V*	*E*	E_{vdW}
Metal/NbS_2	10.021	10.021	11.996	1143.321	-292.314	57.981
TC/NbS_2	10.031	10.031	11.999	1145.666	-292.340	57.980
Metal/$NbSe_2$	10.409	10.409	12.613	1183.352	-254.601	62.016
TTs/$NbSe_2$	10.411	10.411	12.616	1188.573	-254.652	62.015

Table S-4 Geometrical parameters (Å) of CDW and metal phase for bulk 2H-NbS_2 and 2H-$NbSe_2$

	d_1	d_2	d_3	d_4	d_5	d_6
Metal/NbS_2	1.576	1.576	2.846	1.576	1.576	5.998
CDW/NbS_2	1.575	1.575	2.850	1.574	1.574	5.999
Metal/$NbSe_2$	1.691	1.691	2.924	1.691	1.691	6.306
CDW/$NbSe_2$	1.691	1.691	2.927	1.690	1.690	6.308

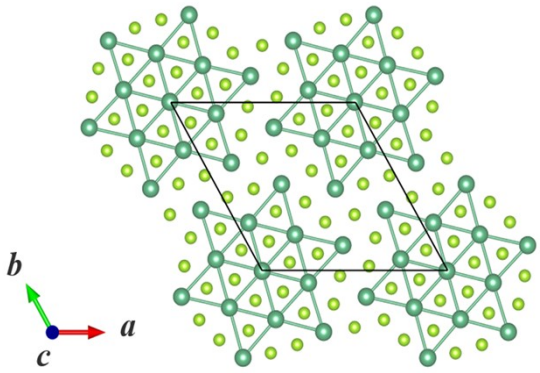

Figure S-1 CDW configuration of monolayer 1T-$NbSe_2$ with a vacuum layer of 20 Å.

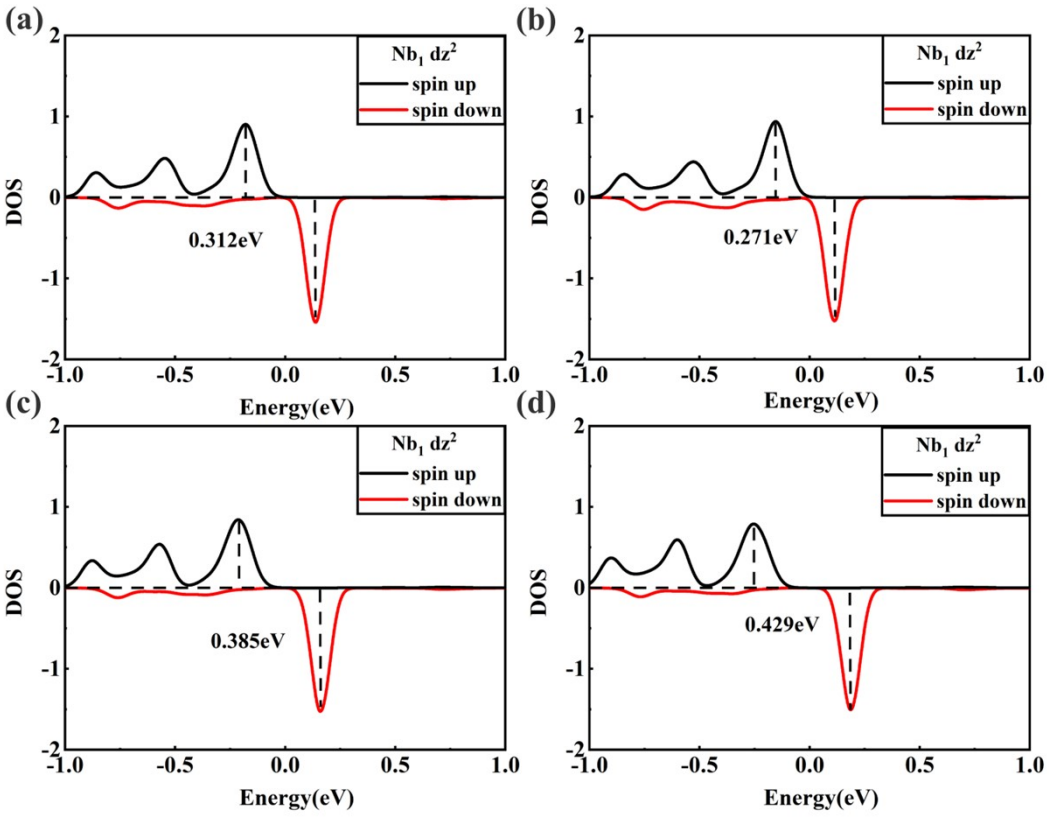

Figure S-2 Motto band gap of CDW configuration of mono-layer 1T-$NbSe_2$ at various U values. (a) U = 1 eV, (b) U = 1.5 eV, (c) U = 2.0 eV, (d) U = 2.5 eV

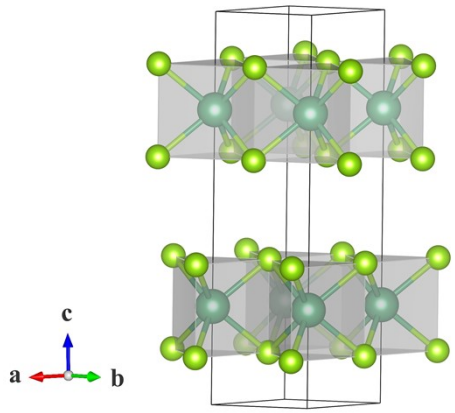

Figure S-3 Crystal structure of 2H-NbX_2 (X= S and Se) bulk. Nb and Se atoms are respectively drawn by dark green and light green balls.

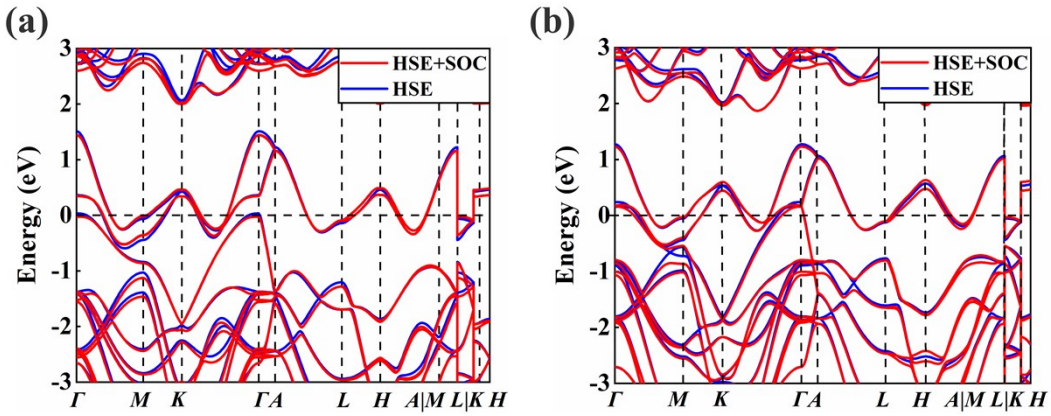

Figure S-4 Energy band of bulk (a) 2H-NbS_2 and (b) 2H-$NbSe_2$. Blue and red lines represent the HSE band without and with SOC calculations, respectively.'

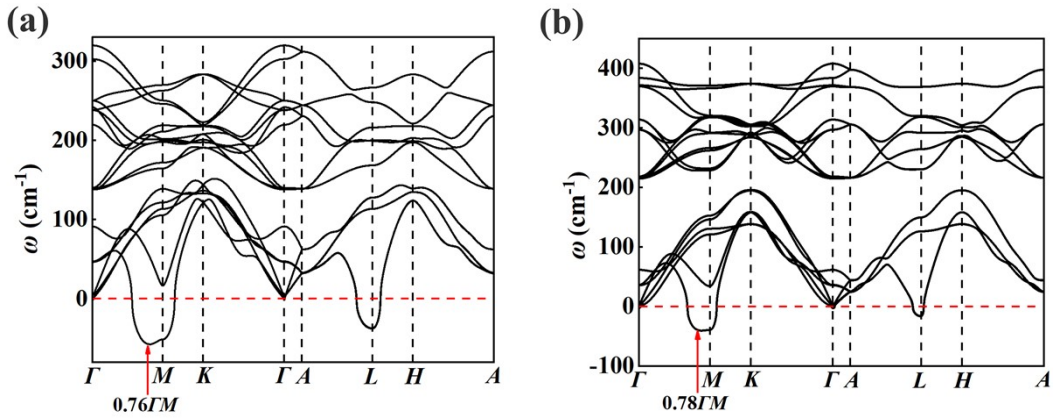

Figure S-5 Phonon dispersion of bulk (a) 2H-NbS_2 and (b) 2H-$NbSe_2$.

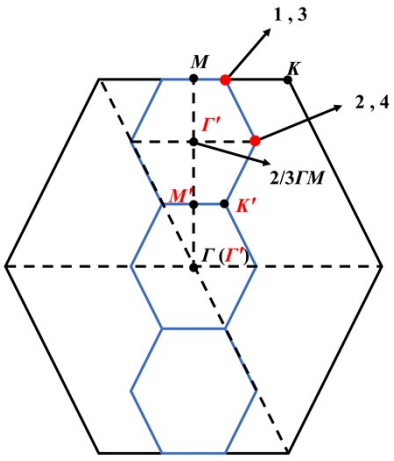

Figure S-6 Brillouin zone of hexagonal NbX_2 (X = S and Se) lattice. The black line represents the undistorted primitive unit cell and blue line represents the unit cell of CDW phase.

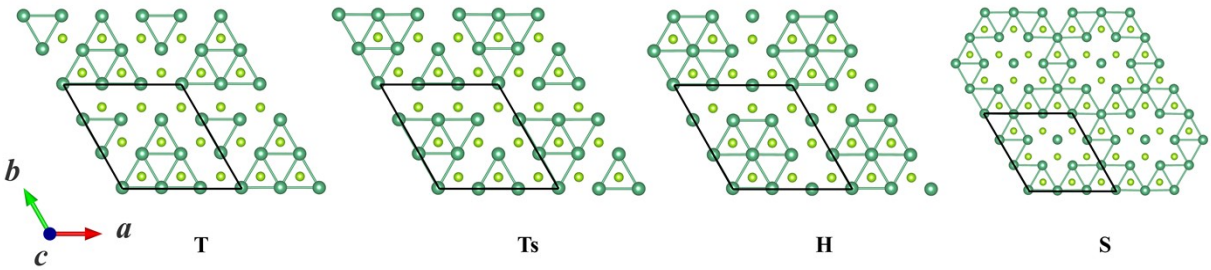

Figure S-7 CDW configurations for mono-layer 1H-NbX_2 (X = S and Se) with a vacuum layer of 20 Å.

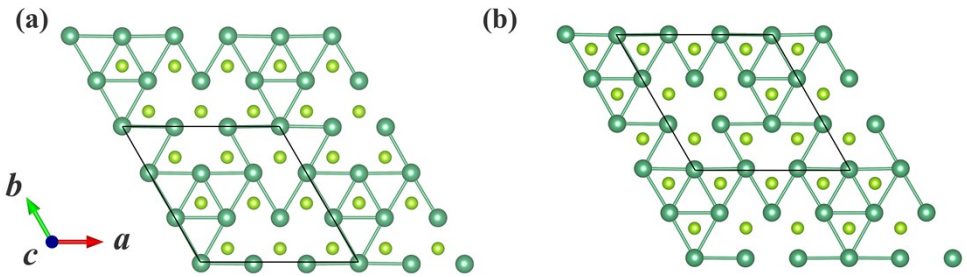

Figure S-8 C (a) and T′ (b) monolayer configuration in the TC bilayer structure for bulk 2H-NbS_2.

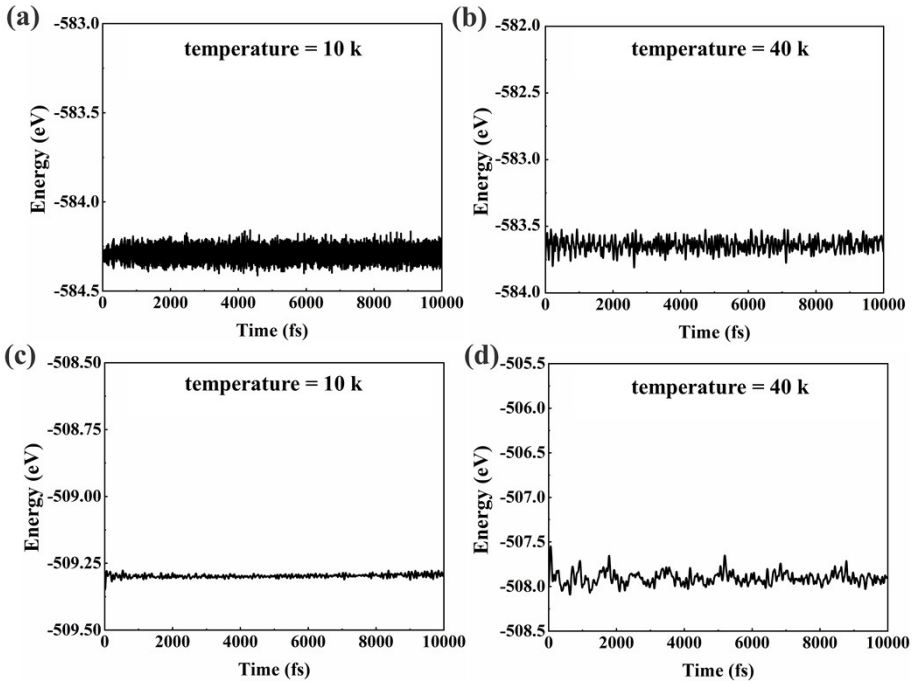

Figure S-9 Molecular dynamics simulation with NVT ensemble. (a-b) TC configuration at 10 K and 40 K for 2H-NbS_2, respectively; (c-d) TTs configuration at 10 K and 40 K for 2H-$NbSe_2$, respectively.

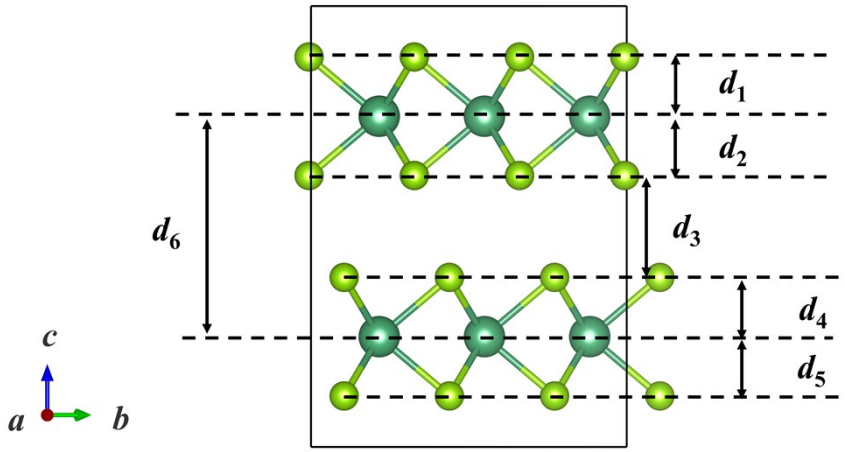

Figure S-10 Schematic diagram of atomic separation of CDW and metal phase for bulk 2H-NbX_2

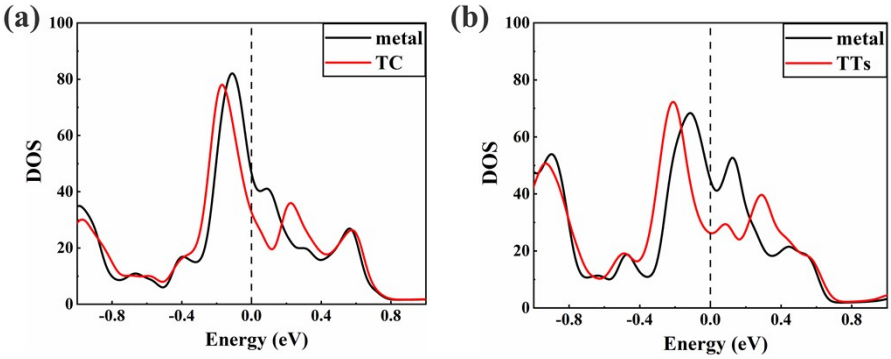

Figure S-11 (a) In-plane DOS of TC configuration and metal phase of bulk 2H-NbS_2. (b) In-plane DOS of TTs configuration and metal phase of bulk 2H-$NbSe_2$.

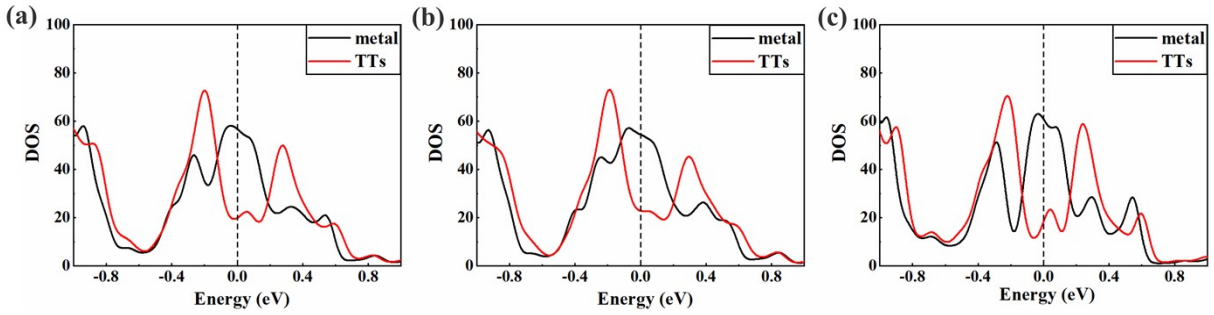

Figure S-12 DOS without vdW interaction for CDW and metal phases of bulk 2H-$NbSe_2$, (a) Total DOS. (b) In-plane DOS. (c) Out-of-plane DOS.

Section 2: Two-band model Theory

Density of states (DOS) is essentially the number of different states that electrons are allowed to occupy at a specific energy level, that is, the number of electronic states per unit energy and unit volume. The bulk properties of conductive solids, such as specific heat, paramagnetic susceptibility, and other transport phenomena, depend on this function. The dispersion relationship between the two energy bands in a semimetal is as follows:

$$E_1(k) = E_1(k_{10}) - \frac{\hbar^2(k-k_{10})^2}{2m_1}, \qquad E_2(k) = E_2(k_{20}) + \frac{\hbar^2(k-k_{20})^2}{2m_2}$$

E_1 (k_{10}) is the top of the first band, E_2 (k_{20}) is the bottom of the second band, and m_1 and m_2 are the effective masses of the two bands. For band 1:

$$Z_1(E) = \frac{2V}{(2\pi)^3}\int \frac{dS}{|\nabla_k E|} = \frac{2V}{(2\pi)^3}\frac{4\pi k^2}{\hbar\sqrt{2\left[E_1(k_{10}) - E_1(k)\right]/m_1}} = \frac{2V}{(2\pi)^2}\left(\frac{2m_1}{\hbar^2}\right)^{3/2}\sqrt{E_1(k_{10}) - E_1(k)}$$

In the same way

$$Z_2(E) = \frac{2V}{(2\pi)^2}\left(\frac{2m_2}{\hbar^2}\right)^{3/2}\left[E_2(k) - E_2(k_{20})\right]^{1/2}$$

In the calculation, we are more concerned about the change of the average number of electrons with energy, that is, the number of electrons in a unit volume per unit energy. According to the Fermi-Dirac distribution function, we can directly write the statistical electron number

$$f(E)Z(E)\mathrm{d}E$$

$f(E)Z(E)$ specifically summarizes the statistical distribution of electrons in the system according to energy, which depends on the Fermi statistical distribution $f(E)$ and the density of states $Z(E)$ as shown in Figure S-13.

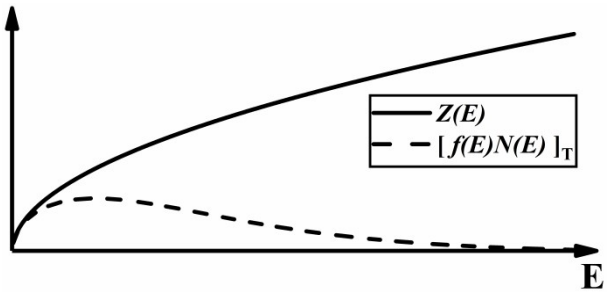

Figure S-13 Free electron density of states (solid line) and electron distribution according to energy (dashed line)

When there are two energy bands with different effective masses in the semimetal, where m_1<m_2, so the energy band 2 is smoother than the energy band 1. If these two energy bands are located in the position of Figure S-14(a), Figure S-14(b) shows the relationship between the DOS of the two energy bands. If only energy band 1 crosses through the Fermi surface, it means that the valence band crosses through the Fermi surface E_{F1}. Part of the electrons in band 1 will transfer to band 2, forming holes in band 1, causing the material to be hole-conducting. If only energy band 2 passes through the Fermi surface E_{F2}, it means that the conduction band has crossed through the Fermi surface, and the unfilled energy level in the conduction band can accommodate more electrons, which is considered to be electronic conduction. In the Figure S-14, the electronic occupation of energy band 2 is stronger than that of energy band 1, which is the result of the change of energy band slope owing to the difference in

effective mass. When two energy bands cross through the Fermi level at the same time as shown in Figure S-14(b), there is both electron conduction and hole conduction in the material. At this time, it is very important to judge whether the material is specifically electrons or holes as carriers. The bulge in Figure S-14(b) is due to the overlap of electrons in the two energy bands. When the Fermi level is located at the bulge E_{F1}, it means that the two energy bands have crossed through the Fermi level. We can observe that the bulge is not symmetrical, and the highest point is more inclined to the place with higher energy. This is because the rising trend of the electron occupation that provides the hole conduction band is greater than the rising trend of the DOS that provides the electron conduction band. Therefore, if the Fermi surface (E_{F1}) is close to the hole energy band, that is, the right side of the bulge (at this time, the slope occupied by electrons is negative value) and d(DOS)/dE< 0, it can be determined that holes are more competitive than electrons, and vice versa.

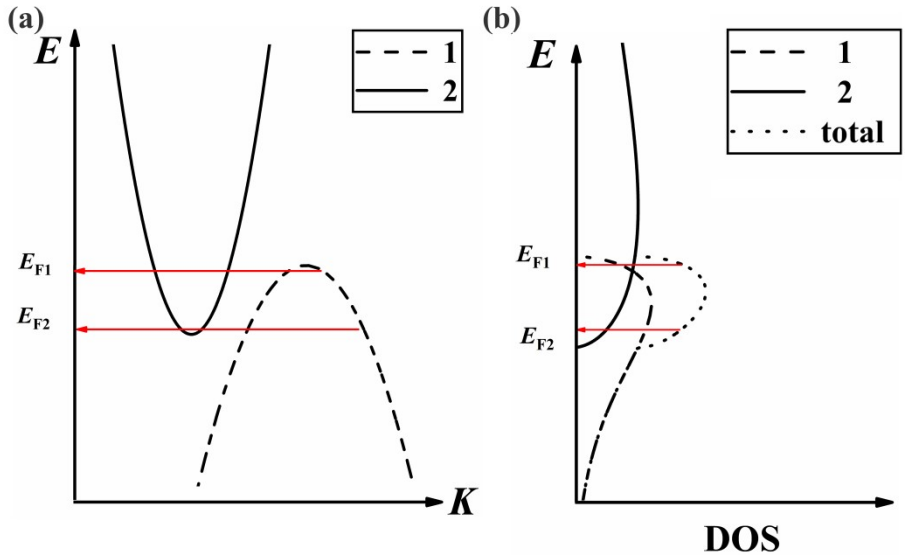

Figure S-14(a) Model of two energy bands in the semimetal. (b) Slope of DOS when Fermi level locate at the top of valence band (E_{F2}) or bottom of conduction band (E_{F1}).

REFERENCE

[1] A. Meerschaut, C. Deudon, Crystal structure studies of the 3R-$Nb_{1.09}S_2$ and the 2H-$NbSe_2$ compounds: correlation between nonstoichiometry and stacking type (= polytypism), Materials Research Bulletin, 36 (2001) 1721-1727.

[2] F. Jellinek, G. Brauer, H. MÜLler, Molybdenum and Niobium Sulphides, Nature, 185 (1960) 376-377.

[3] S. F. Meyer, R. E. Howard, G. R. Stewart, J. V. Acrivos, T. H. Geballe, Properties of intercalated 2H-$NbSe_2$, 4Hb-TaS_2, and 1T-TaS_2 The Journal of Chemical Physics, 62 (2008) 4411-4419.

[4] C. J. Carmalt, T. D. Manning, I. P. Parkin, E. S. Peters, A. L. Hector, Formation of a new (1T) trigonal NbS_2 polytype via atmospheric pressure chemical vapour deposition, Journal of Materials Chemistry, 14 (2004) 290-291.